Research Square

Preprints are preliminary reports that have not undergone peer review.
They should not be considered conclusive, used to inform clinical practice,
or referenced by the media as validated information.

Flow cytometry-assisted bioprocess optimization of Heterocapsa pygmaea for enhanced cell growth and PCP-associated fluorescence

Jiang-Ting Lu Chen
National Taiwan Ocean University
Chi-Cheng Huang
National Taiwan Ocean University
Hung-Yun Lin
National Taiwan Ocean University
Jin-De Li
China Medical University
Yi-Jung Chen
National Taiwan Ocean University
Fat-Tin Agassi Sze
National Taiwan Ocean University
Yen-Ling Chen
National Taiwan Ocean University
Fan-Hua Nan
National Taiwan Ocean University
Mary Joy Libatique-Asprec
Isabela State University
Meng-Chou Lee
mengchoulee@email.ntou.edu.tw

National Taiwan Ocean University

Research Article

Keywords: dinoflagellate, Heterocapsa pygmaea, peridinin–chlorophyll a protein, culture optimization, flow cytometry, bioprocess optimization

Posted Date: July 31st, 2026

DOI: https://doi.org/10.21203/rs.3.rs-10235386/v1

License: This work is licensed under a Creative Commons Attribution 4.0 International License.
Read Full License

Additional Declarations: No competing interests reported.

Abstract

Graphical abstract Highlight Culture conditions for Heterocapsa pygmaea were optimized using RSM. The modified C5 medium significantly enhanced biomass and PCP performance. Flow cytometry enabled rapid in vivo tracking of PCP physiological status. FCM offers a scalable strategy for real-time PCP monitoring during extraction. Authentic PCP complexes with molecular weights of 10–15 kDa were confirmed. ABSTRACT Dinoflagellates are promising sources of high-value light-harvesting proteins; however, their commercial utilization remains limited by insufficient optimization of cultivation conditions and the lack of efficient physiological monitoring tools. This study developed a cultivation and monitoring framework to enhance biomass productivity and peridinin–chlorophyll a–protein (PCP) performance in Heterocapsa pygmaea. PCP was characterized using SDS-PAGE and HPLC, confirming a molecular weight of 10–15 kDa and a pigment composition dominated by peridinin and chlorophyll a. Systematic evaluation of environmental (temperature and light intensity) and nutritional (phosphorus, nitrogen, and iron) factors identified optimal cultivation conditions as 24 °C, 100 μmol photons m^{-2} s^{-1}, 60 μM phosphorus supplied as mixed sources, nitrate or mixed nitrogen conditions, and 17.55 μM iron. Flow cytometry enabled the simultaneous assessment of cell density and intracellular fluorescence intensity, providing a rapid in vivo indicator of PCP-associated physiological performance across cultivation treatments. Incorporation of the optimized parameters into a modified C5 medium significantly improved biomass productivity and fluorescence responses compared with conventional f/2 and K media ($p < 0.05$). These findings demonstrate that combining cultivation optimization with flow cytometry-guided physiological monitoring is an effective strategy for improving PCP production in H. pygmaea. This study establishes a scalable framework for the cultivation of PCP-producing dinoflagellates and highlights the broader potential of flow cytometry-assisted monitoring for microalgal bioprocess development and industrial biotechnology applications.

Highlights

- Culture conditions for *Heterocapsa pygmaea* were optimized using RSM.
- The modified C5 medium significantly enhanced biomass and PCP performance.
- Flow cytometry enabled rapid *in vivo* tracking of PCP physiological status.
- FCM offers a scalable strategy for real-time PCP monitoring during extraction.
- Authentic PCP complexes with molecular weights of 10–15 kDa were confirmed.

INTRODUCTION

Dinoflagellates are ecologically important microalgae that contribute substantially to marine primary productivity and biogeochemical cycling. Beyond their ecological roles, they have emerged as a promising source of high-value biomolecules, particularly light-harvesting pigment–protein complexes with distinctive optical and functional properties. Among these, the peridinin–chlorophyll *a*–protein (PCP) complex is of particular interest because of its high fluorescence quantum yield, broad excitation

spectrum, and near-unity energy transfer efficiency, which make it highly suitable for applications in fluorescence-based diagnostics, biosensing, and photonic systems (Qiu et al., 2023; Schulte et al., 2025).

Despite its significant biotechnological potential, the practical use of PCP remains constrained by the lack of efficient and scalable production systems. Previous studies have primarily focused on the structural and photophysical characterization of PCP, particularly in model dinoflagellates such as *Amphidinium carterae*, whereas comparatively little attention has been paid to species such as *Heterocapsa pygmaea*, which possess distinct PCP forms and pigment compositions (Niedzwiedzki et al., 2013; Carbonera et al., 2014). More importantly, few studies have integrated cultivation optimization with functional performance assessment, creating a gap between laboratory characterization and scalable process development.

Microalgal growth and pigment synthesis are strongly regulated by environmental conditions, such as temperature and light intensity, as well as nutrient availability, particularly nitrogen, phosphorus, and iron. These factors influence photosynthetic efficiency, metabolic activity, and pigment accumulation through interconnected physiological pathways (Kana et al., 1997; Yamashita et al., 2026). However, dinoflagellates exhibit species-specific physiological plasticity, including flexible nutrient acquisition strategies and dynamic pigment regulation, which complicates the identification of optimal cultivation conditions. Consequently, many existing studies rely on single factor optimization or endpoint analyses that do not fully capture interactions among variables during cultivation.

In addition to cultivation constraints, conventional PCP quantification methods further limit process development. Extraction-based techniques can provide absolute pigment or protein concentrations, but they are labor-intensive, time-consuming, and poorly suited to repeated monitoring across multiple experimental conditions. These limitations reduce analytical throughput and slow down optimization workflows. Recent advances in microalgal biotechnology have therefore emphasized the value of high-throughput physiological screening tools that can more efficiently link culture conditions with intracellular responses.

Flow cytometry (FCM) has emerged as a powerful analytical platform for single-cell analysis of microalgal systems, enabling the simultaneous quantification of cell density and intracellular fluorescence signatures (Černterová and Galbraith, 2021; Di Caprio et al., 2021). In PCP-producing dinoflagellates, these fluorescence signatures provide an informative indicator of intracellular pigment status and photosynthetic function without requiring destructive extraction procedures. This capability enables flow cytometry-guided PCP monitoring and allows rapid comparison of culture performance across multiple environmental and nutritional conditions. Compared with conventional quantification approaches, FCM offers a scalable strategy for dynamic physiological screening and accelerated process optimization.

From a bioprocess engineering perspective, integrating analytical monitoring with cultivation optimization is increasingly recognized as an effective strategy for accelerating the development of scalable microalgal production systems. Recent advances in microalgal biotechnology have emphasized

the use of physiological indicators, sensor-based monitoring, and high-throughput analytical platforms to rapidly evaluate culture performance under multiple environmental and nutritional conditions (Novoveská et al., 2023; Dębowski et al., 2025). Such approaches improve process efficiency by enabling data-driven optimization and reducing the time required for experimental screening. Despite these advances, comparable integrated cultivation-monitoring frameworks remain limited in dinoflagellate systems, particularly among PCP-producing species.

H. pygmaea is a promising yet underutilized dinoflagellate species because of its ability to produce PCP with favorable fluorescence properties. Its cultivation requirements and PCP production dynamics remain poorly understood, and no study has yet established a framework that simultaneously optimizes the species' biomass productivity and PCP-associated functional performance.

Therefore, the present study aimed to (i) characterize the molecular and pigment composition of PCP from *H. pygmaea* and (ii) establish an integrated cultivation optimization framework through the systematic evaluation of environmental (temperature and light) and nutritional (nitrogen, phosphorus, and iron) factors affecting biomass productivity and PCP-associated fluorescence performance. A central feature of this work is the use of flow cytometry-guided monitoring as an *in vivo* analytical platform for the simultaneous assessment of biomass productivity and PCP-associated fluorescence responses. By combining cultivation optimization with physiological signal tracking, this study establishes an integrated dinoflagellate bioprocess optimization framework for enhanced PCP production. These findings provide biological and bioprocess insights into *H. pygmaea* cultivation while demonstrating the value of flow cytometry-guided physiological monitoring for accelerating the development of a PCP-oriented microalgal process.

MATERIALS AND METHODS

2.1 Microalgal strain and culture conditions

The dinoflagellate *Heterocapsa pygmaea* (K-0961) was obtained from the Norwegian Culture Collection of Algae (NORCCA, Norway) and maintained under controlled laboratory conditions. Cultures were grown in sterilized seawater (30 ppt salinity) supplemented with K medium (Keller et al., 1987).

All cultures were incubated at 24°C under LED T8 white light at an intensity of 100 µmol photons m^{-2} s^{-1} with a 12:12 h light: dark photoperiod. Stock cultures were maintained in the exponential growth phase and used for subsequent experiments. The initial inoculation density was standardized at approximately 1.0×10^5 cells mL^{-1}.

2.2 PCP characterization

2.2.1 Protein molecular weight determination

The molecular weight of peridinin–chlorophyll *a*–protein (PCP) was determined by SDS-PAGE. Protein samples (1 μg) were mixed with 5× loading buffer and denatured at 95°C for 10 min. Electrophoresis was performed using a 15% polyacrylamide gel at 80 V for stacking, followed by 100 V for separation. Protein bands were visualized by Coomassie Brilliant Blue staining and compared with a prestained molecular weight marker.

2.2.2 Pigment composition analysis

The pigment composition of PCP was analyzed using high-performance liquid chromatography (HPLC). Algal biomass was harvested by centrifugation and extracted using acetone:methanol (7:2, v/v) with bead-assisted cell disruption. Extracts were filtered through 0.2 μm PTFE syringe filters prior to analysis. HPLC separation was performed using a reverse-phase C18 column with gradient elution under controlled flow conditions. Pigments were detected at 475 nm and 665 nm to identify peridinin and chlorophyll a, respectively.

2.3 Experimental design for integrated culture optimization

A sequential optimization framework was employed to systematically evaluate the individual and combined effects of environmental and nutritional variables on culture productivity and PCP-associated fluorescence responses in *H. pygmaea*. Optimization experiments were designed to identify cultivation conditions that maximized both biomass yield and fluorescence-based cellular responses while maintaining physiological stability. All experiments were conducted in sterilized seawater (30 ppt) using K medium as the basal medium, unless otherwise specified.

Cultures were grown in Erlenmeyer flasks (200–400 mL working volume) under a 12:12 h light: dark photoperiod with continuous aeration. Each treatment was conducted in quadruplicate (n = 4), with an initial inoculation density of approximately 1.0×10^5 cells mL^{-1}. The experiments were carried out over 8 days, with sampling performed on days 0, 2, 4, 6, and 8.

2.3.1 Temperature optimization

Cultures were incubated at 16, 20, 24, and 28°C under 60 μmol photons m^{-2} s^{-1} to evaluate the effects of temperature on growth. Cell density and specific growth rate (SGR) were measured on days 0 and 8. Response surface methodology (RSM) was used to determine the optimal temperature conditions.

2.3.2 Light intensity optimization

Following temperature optimization, cultures were exposed to light intensities of 20, 60, 100, and 140 μmol photons m^{-2} s^{-1} at 24°C. Growth and fluorescence responses were monitored, and optimal irradiance conditions were identified using RSM.

2.3.3 Phosphorus optimization

(a) Concentration

Phosphorus concentrations of 10, 30, 60, and 120 μM were tested under optimal temperature and light conditions. Samples were collected every two days to measure cell density, relative fluorescence intensity, and pH. Total phosphorus in the medium was also analyzed to assess nutrient utilization.

(b) Source

Phosphorus sources included inorganic ($NaH_2PO_4 \cdot 2H_2O$), organic (Na_2β-glycerophosphate), and mixed (1:1) forms. All treatments were standardized to equivalent phosphorus levels.

2.3.4 Nitrogen optimization

(a) Comparison of nitrogen sources

Nitrogen sources (nitrate, ammonium, and urea) were evaluated at equivalent nitrogen concentrations.

(b) Nitrogen substitution strategy

A mixed nitrogen treatment (50% nitrate + 50% urea) was tested to assess whether a cost-effective substitution could be achieved without compromising performance.

2.3.5 Iron optimization

Iron concentrations of 0, 1.46, 2.93, 5.85, 11.7, and 17.55 μM were tested. Growth performance, fluorescence, and pH were monitored every 2 days. RSM analysis was applied to determine the optimal iron level.

2.3.6 Integrated medium formulation and validation

Based on the optimal conditions, a modified culture medium (C5) was developed. Its performance was compared with that of conventional f/2 and K media under identical conditions. Growth, SGR, and PCP-associated fluorescence were monitored by flow cytometry.

2.4 Flow cytometry-based analysis

Flow cytometry (Attune™ NxT, Thermo Fisher Scientific) was used to quantify cell density and PCP-associated fluorescence. Samples (200 μL) were analyzed at a flow rate of 200 μL min^{-1} using a 488 nm excitation laser.

Cells were gated using forward scatter (FSC) and side scatter (SSC) distributions to distinguish viable algal populations from debris and non-cellular particles. A minimum of 10,000 events was acquired per sample. Fluorescence signals associated with PCP were detected in the PerCP-A channel (695/40 nm) under 488 nm laser excitation. Instrument settings were maintained constant throughout all analyses to ensure comparability among treatments. Relative fluorescence intensity values were normalized to gated populations and expressed in arbitrary fluorescence units. Representative fluorescence histograms generated during optimization experiments are provided in the Supplementary Materials (Figures S1–S7).

The following parameters were calculated:

- Cell density (cells mL^{-1})
- Relative fluorescence intensity (PCP-associated fluorescence proxy)
- Specific growth rate (SGR; % day^{-1}):

SGR was calculated as follows:

$$\mathbf{SGR = [(\ln N_2 - \ln N_1) / (t_2 - t_1)] \times 100}$$

where $\mathbf{N_1}$ and $\mathbf{N_2}$ represent the initial and final cell densities (cells mL^{-1}), respectively, and $\mathbf{(t_2 - t_1)}$ represents the cultivation period in days.

2.5 Rationale for flow cytometry-based productivity assessment

Flow cytometry (FCM) was employed as a primary analytical tool because it enables rapid, high-throughput analysis of microalgal cultures at single-cell resolution. Conventional extraction-based quantification of pigment–protein complexes, although capable of providing absolute concentrations (e.g., mg L^{-1}), is labor-intensive and limits analytical throughput (Černterová & Galbraith, 2021).

Recent studies have demonstrated that fluorescence-based measurements obtained through FCM provide valuable indicators of intracellular pigment status, physiological condition, and stress-associated cellular responses in microalgae, supporting their use in rapid cultivation assessment and process optimization (Hyka et al., 2013; Černterová & Galbraith, 2021; Dębowski et al., 2025).

In this study, fluorescence signals associated with PCP were used as relative indicators of functional performance across culture conditions. This approach enables efficient screening of environmental and nutritional parameters and rapid process optimization. While absolute PCP quantification remains important for downstream validation, FCM provides a scalable and effective strategy for early stage optimization.

2.6 Supporting analyses

2.6.1 Total phosphorus analysis

Total phosphorus was determined by the molybdenum blue method following persulfate digestion, with absorbance measured at 880 nm.

2.6.2 pH measurement

Culture pH was monitored throughout cultivation using a calibrated digital pH meter to assess changes associated with nutrient assimilation and photosynthetic carbon fixation.

2.7 Statistical and optimization analysis

All data were expressed as mean ± standard deviation (n = 4). Normality and homogeneity of variance were assessed before analysis using standard diagnostic tests. Differences among treatments were evaluated using one-way analysis of variance (ANOVA), followed by Tukey's honestly significant difference (HSD) post hoc test for multiple comparisons. Statistical significance was accepted at $p < 0.05$. RSM analysis was performed using Design-Expert software (v12.0) to evaluate the relationships among environmental variables and culture responses. Quadratic polynomial models were generated, and model adequacy was assessed using ANOVA, regression coefficients (R^2), and lack-of-fit analysis. Optimal conditions were predicted based on the maximization of biomass productivity and fluorescence responses.

RESULTS

3.1 Characterization of peridinin–chlorophyll *a*–protein (PCP)

The protein extracted from *H. pygmaea* was characterized to confirm its identity as peridinin–chlorophyll a–protein (PCP). SDS-PAGE analysis revealed a distinct protein band at approximately 10–15 kDa (Fig. 1A). HPLC analysis further confirmed the pigment composition of the complex, where a major peridinin peak was detected at 475 nm (~ 10.5 min retention time), and chlorophyll a was identified at 665 nm (~ 48.0 min) (Fig. 1B).

3.2 Flow cytometry-based assessment of biomass and PCP-associated performance

Flow cytometry (FCM) enabled the simultaneous quantification of cell density and relative fluorescence intensity in H. pygmaea. Distinct algal populations were clearly resolved by FSC–SSC discrimination, allowing reliable separation of viable cells from debris. Fluorescence histograms obtained from the BL3-A (PerCP-associated) channel showed stable intracellular pigment-associated signals, while sequential gating and microscopic validation confirmed the accurate identification of viable H. pygmaea cells and the exclusion of background particles (Fig. 2). Across treatments, fluorescence profiles closely paralleled biomass productivity. Importantly, FCM also captured transient responses, showing a temporary fluorescence suppression under excess phosphorus and elevated iron conditions. Representative flow cytometry fluorescence histograms illustrate treatment-dependent shifts in intracellular fluorescence signals under different temperatures and light conditions (Supplementary Figures S1–S7).

3.3 Effects of temperature and light intensity on biomass productivity

Temperature significantly affected the growth of H. pygmaea. After 8 days, both cell density and specific growth rate (SGR) were highest at 24°C (Fig. 3A–B), and response surface analysis confirmed

approximately 24°C as the thermal optimum (Fig. 3E–F). Conversely, reduced growth was observed at 16°C and higher temperatures. Light intensity similarly influenced biomass productivity. Cultures exposed to 60–140 μmol photons m^{-2} s^{-1} showed significantly greater biomass productivity than low-light treatments, with maximal productivity achieved at 100 μmol photons m^{-2} s^{-1} (Fig. 3C, G–H). While SGR remained stable across light treatments (Fig. 3D), fluorescence intensity increased under optimal irradiance.

3.4 Effects of phosphorus concentration and source on biomass and PCP-associated performance

Phosphorus availability strongly influenced culture productivity and fluorescence responses in H. pygmaea. Cultures supplied with 60 μM phosphorus showed the highest biomass yield and SGR (Fig. 4A–B). Cell density over the cultivation period demonstrated better growth at intermediate phosphorus concentrations than under deficient (10 μM) or excess (120 μM) phosphorus treatments (Fig. 4C). Low-phosphorus treatments rapidly depleted available phosphorus, whereas residual accumulation at 120 μM indicated reduced utilization efficiency under excess supply (Fig. 4F). Under excess phosphorus (120 μM), a transient decline in fluorescence intensity was observed (Fig. 4D). Among the phosphorus source treatments, mixed phosphorus (MP) treatments produced the highest fluorescence responses (Fig. 4G).

3.5 Effects of nitrogen source and nitrate–urea substitution on biomass and PCP-associated performance

Nitrogen source significantly influenced biomass productivity and fluorescence responses in H. pygmaea. Nitrate and mixed nitrogen treatments produced the highest cell densities and SGR (Fig. 5A–B). Ammonium-dominated treatments showed significantly reduced biomass and fluorescence responses (Fig. 5A–C). Urea-supported cultures showed similar but less pronounced reductions. The nitrogen source also influenced culture pH, with ammonium-containing treatments showing greater pH variation than nitrate-based treatments (Fig. 5D). Notably, partial replacement of nitrate with urea (mixed nitrogen strategy) maintained high biomass productivity and fluorescence performance (Fig. 5E–G).

3.6 Effects of iron concentration on biomass and PCP-associated performance

Iron supplementation significantly enhanced biomass productivity and PCP-associated fluorescence responses in H. pygmaea, with optimal performance observed at 17.55 μM iron (Fig. 6A–D, F). Both cell density and specific growth rate increased with iron supplementation up to the optimal concentration, and response surface analysis confirmed enhanced culture productivity under intermediate iron availability (Fig. 6A–D). Conversely, iron limitation constrained growth performance. Relative fluorescence intensity was highest under optimal iron supplementation (17.55 μM), but temporary fluorescence suppression was observed at elevated iron concentrations followed by a subsequent

restoration of fluorescence responses (Fig. 6F). Culture pH remained stable across treatments throughout cultivation (Fig. 6E).

3.7 Validation of optimized conditions using modified C5 medium

Integration of optimized environmental and nutritional parameters into the modified C5 medium significantly enhanced biomass productivity and relative fluorescence intensity compared with conventional f/2 and K media (Fig. 7A–C). Relative fluorescence intensity closely paralleled biomass productivity across the three media (Fig. 7C), and representative fluorescence histograms comparing the modified C5 medium with conventional culture media are presented in Supplementary Figure S7. Culture pH remained stable across media formulations throughout cultivation (Fig. 7D).

DISCUSSION

4.1 Molecular and Pigment Signatures of PCP in Heterocapsa pygmaea

The confirmation of a 10–15 kDa protein band via SDS-PAGE and the identification of peridinin and chlorophyll a as the major chromophores via RP-HPLC align with previous structural reports of PCP complexes in dinoflagellates (Govind et al., 1990; Qiu et al., 2023; Schulte et al., 2025). These individual pigments function as the principal light-harvesting components responsible for expanding the absorption spectrum under blue-green wavelengths, which are predominant in marine environments (Prézelin & Haxo, 1976; Hofmann et al., 1996). The structural integrity observed in the extracted complex underscores the feasibility of using H. pygmaea as a viable bioresource for industrial or diagnostic fluorescent probes.

4.2 Flow Cytometry as an In Vivo Real-Time Monitoring Tool

Compared with conventional extraction-based quantification methods, which are inherently destructive, labor-intensive, and limit screening throughput, the established FCM framework provides a rapid, single-cell analytical platform for process optimization (Černterová & Galbraith, 2021). The close parallel between biomass accumulation and intracellular PerCP fluorescence signals validates the use of cytometric fluorescence as a practical proxy for real-time tracking of functional PCP accumulation. Furthermore, the detection of transient fluorescence variations during nutrient stress underscores the sensitivity of FCM in identifying sub-lethal physiological adjustments before bulk changes in biomass become apparent (Hyka et al., 2013; Jiao et al., 2017; Liu et al., 2024).

4.3 Environmental Regulation of Biomass Productivity

The optimization of physical factors revealed that H. pygmaea exhibits typical physiological boundaries observed in marine dinoflagellates. The optimal thermal setting of 24°C supports balanced metabolic activity, whereas lower temperatures (16°C) restrict enzyme kinetics and higher temperatures induce cellular stress that disrupts growth pathways (Trigueros & Orive, 2001; Yamashita et al., 2026). Similarly, the light intensity optimum of 100 µmol photons m^{-2} s^{-1} represents a saturation threshold where energy generation via photochemical pathways is maximized without provoking photoinhibition or reactive oxygen species (ROS) accumulation typically driven by excessive irradiance (Shen et al., 2016; Zhang et al., 2022).

4.4 Macronutrient Assimilation Dynamics (Phosphorus and Nitrogen)

Phosphorus and nitrogen are essential building blocks for microalgal cell division and pigment-protein synthesis. The high performance observed at 60 µM phosphorus reflects an equilibrium where cellular energy transfer (ATP synthesis) is fully supported without incurring the metabolic stress or economic inefficiency associated with excess accumulation (Huang et al., 2023). The preference for mixed phosphorus sources suggests that H. pygmaea can simultaneously activate inorganic uptake mechanics and organic pathways (such as alkaline phosphatase-mediated hydrolysis) to maximize nutrient-use efficiency (Oh et al., 2010).

Regarding nitrogen, the superior performance supported by nitrate and nitrate-urea mixtures demonstrates steady assimilation kinetics. Although nitrate assimilation requires sequential enzymatic reduction via nitrate and nitrite reductases, the optimized irradiance provided sufficient reducing power to meet this energetic demand (Dagenais-Bellefeuille & Morse, 2013). In contrast, ammonium-dominated cultures suffered from intracellular accumulation and associated oxidative stress, a common toxicity syndrome in microalgae that alters proton balance and destabilizes the medium pH (Salbitani & Carfagna, 2021; Wang & Coyne, 2024). The success of the nitrate-urea substitution highlights a practical strategy for reducing formulation costs in large-scale bioprocesses.

4.5 Micronutrient Impacts and Bioprocess Validation

The strong response to iron supplementation up to 17.55 µM highlights the role of iron as an indispensable cofactor for electron transport chains (PSI and PSII), ferredoxin, and nitrogen-assimilating enzymes (Hurd et al., 2014; Schoffman et al., 2016). The transient suppression of fluorescence under excess iron reflects a classic cellular redox adjustment to counter temporary ROS generation, followed by physiological acclimation (Danouche et al., 2022).

The superior performance of the modified C5 medium validates this integrated approach. By avoiding single-factor optimization bias and simultaneously tuning temperature, irradiance, macro-, and micronutrients, the C5 medium achieves metabolic synergy. Enhanced growth was seamlessly coupled with elevated light-harvesting efficiency, presenting a scalable and highly efficient framework for dinoflagellate-based biotechnology.

4.6 Integration and Validation of the Optimized Bioprocess Conditions

These results confirm that coordinated optimization of temperature, light, phosphorus, nitrogen, and iron substantially improves culture productivity and PCP-associated cellular responses in H. pygmaea. The superior performance of C5 resulted from improved coordination among phosphorus metabolism, nitrogen assimilation, and photosynthetic electron transport: adequate phosphorus supported ATP production and cell division, nitrate-dominant conditions stabilized nitrogen metabolism, and elevated iron enhanced electron transport efficiency (Hurd et al., 2014; Schoffman et al., 2016). This concordance between biomass accumulation and fluorescence responses further supports the usefulness of flow cytometry-guided monitoring for the rapid assessment of culture performance during process optimization. The stability of culture pH across media formulations further suggests that the improved performance of the modified C5 medium was primarily associated with an optimized nutrient composition rather than with substantial differences in culture chemistry. Collectively, this study establishes an integrated dinoflagellate bioprocess optimization framework that combines environmental and nutritional optimization with real-time fluorescence-based physiological assessment. This approach provides a scalable strategy for PCP production and highlights the broader application of FCM-guided monitoring in microalgal biotechnology and industrial bioprocess development.

CONCLUSION

This study demonstrates that optimizing environmental and nutritional parameters significantly enhanced biomass productivity and PCP-associated fluorescence responses in *H. pygmaea*. Optimal cultivation conditions were identified as 24°C, 100 µmol photons m^{-2} s^{-1}, 60 µM phosphorus supplied from mixed sources, nitrate, or mixed nitrogen conditions, and 17.55 µM iron. Under these conditions, the modified C5 medium consistently outperformed conventional f/2 and K media in supporting growth and PCP-associated physiological performance.

Biochemical characterization confirmed the presence of authentic PCP complexes, with SDS-PAGE and HPLC analyses revealing the characteristic molecular weight and a pigment composition dominated by peridinin and chlorophyll *a*. Flow cytometry proved to be an effective in vivo monitoring platform, enabling rapid assessment of biomass productivity and PCP-associated fluorescence responses under multiple cultivation conditions.

By combining cultivation optimization with fluorescence-based physiological monitoring, this study establishes a practical framework for improving PCP production in *H. pygmaea*. These findings provide a foundation for the scalable cultivation of PCP-producing dinoflagellates and demonstrate the broader value of flow cytometry-guided monitoring as a high-throughput tool for microalgal bioprocess development and industrial biotechnology.

Declarations

Competing Interests

The authors declare they have no competing financial or non-financial interests directly or indirectly related to this work within the past 3 years.

Ethics approval

Not applicable. This study does not involve human participants, data, or biological materials, nor does it involve any animal subjects

Consent to participate

Not applicable.

Consent to publish

Not applicable.

Funding

The authors declare that no external funding, grants, or financial support were received for the research, authorship, and/or publication of this article.

Author Contribution

Conceptualization: J.-T. L .C, C.-C.H, M.-C. L ; Methodology: J.-T. L .C, C.-C. H , H.-Y. L ; Formal analysis and investigation: J.-T. L .C, C.-C.H, Y.-J. C, F.-T.A.S, Y.-L.C ; Writing - original draft preparation: M.J.L.-A, J.-D.L ; Writing - review and editing: F.-H.N, M.J.L.-A,M.-C. L, J.-D.L ; Funding acquisition: Not applicable ; Resources: M.-C.L ; Supervision: M.J.L.-A,M.-C. L. All authors read and approved the final manuscript.

Acknowledgement

The authors sincerely thank the Algal Cultivation and Biotech Laboratory for their invaluable technical assistance and support throughout this study. We also gratefully acknowledge the Norwegian Culture Collection of Algae (NORCCA, Norway) for providing the microalgal strain (Heterocapsa pygmaea) used in this research.

Data Availability

All data supporting the findings of this study are available within the article and its supplementary materials. The microsatellite primer sequences and raw reference data describing the microsatellites

used in this study are listed in Supplementary Table 2.

ACKNOWLEDGEMNTS

The authors sincerely thank the Algal Cultivation and Biotech Laboratory for their invaluable technical assistance and support throughout this study. We also gratefully acknowledge the Norwegian Culture Collection of Algae (NORCCA, Norway) for providing the microalgal strain (*Heterocapsa pygmaea*) used in this research.

References

1. Carbonera D, Di Valentin M, Spezia R, Mezzetti A (2014) The unique photophysical properties of Peridinin–chlorophyll a–protein. *Curr Protein Pept Sci* 15:332–350.
2. Dagenais-Bellefeuille S, Morse D (2013) Putting the N in dinoflagellates. *Front Microbiol* 4:369.
3. Danouche M, El Ghatchouli N, Arroussi H (2022) Overview of the management of heavy metals toxicity by microalgae. *J Appl Phycology* 34:475–488.
4. Di Caprio F, Posani S, Altimari P, Concas A, Pagnanelli F (2021) Single cell analysis of microalgae and associated bacteria flora by using flow cytometry. *Biotechnol Bioprocess Eng* 26:898–909. https://doi.org/10.1007/s12257-021-0054-9
5. Doucette GJ, Harrison PJ (1991) Aspects of iron and nitrogen nutrition in the red tide dinoflagellate *Gymnodinium sanguineum. Mar Biol* 110:165–173.
6. Dębowski M, Kazimierowicz J, Zieliński M (2025) Multi-sensing monitoring of the microalgae biomass cultivation systems for biofuels and added value products synthesis—Challenges and opportunities. *Appl Sci* 15:7324. https://doi.org/10.3390/app15137324
7. Govind NS, Roman SJ, Iglesias-Prieto R, Trench RK, Triplett EL, Prézelin BB (1990) An analysis of the light-harvesting Peridinin–chlorophyll a–protein from dinoflagellates by immunoblotting techniques. *Proc R Soc Lond B Biol Sci* 240:187–195.
8. He H, Chen F, Li H, Xiang WZ, Li Y, Jiang Y (2010) Effect of iron on growth, biochemical composition and paralytic shellfish poisoning toxins production of *Alexandrium tamarense. Harmful Algae* 9:98–104.
9. Hofmann E, Wrench PM, Sharples FP, Hiller RG, Welte W, Diederichs K (1996) Structural basis of light harvesting by carotenoids: peridinin-chlorophyll-protein from *Amphidinium carterae. Science* 272:1788–1791.
10. Huang XL, Zhuang YQ, Xiong YY, Li DW, Ou LJ (2023) Efficient modulation of cellular phosphorus components in response to phosphorus deficiency in the dinoflagellate *Karenia mikimotoi*. *Appl Environ Microbiol* 89:e0086723.
11. Hurd CL, Harrison PJ, Bischof K, Lobban CS (2014) Nutrients. In: Seaweed ecology and physiology, 2nd edn. *Cambridge University Press, Cambridge* pp 238–293.

12. Hyka P, Lickova S, Přibyl P, Melzoch K, Kovar K (2013) Flow cytometry for the development of biotechnological processes with microalgae. *Biotechnol Adv* 31:2–16.
13. Jiao Y, Ouyang HL, Jiang YJ, Kong XZ, He W, Liu WX, Yang B, Xu FL (2017) Effects of phosphorus stress on the photosynthetic and physiological characteristics of *Chlorella vulgaris* based on chlorophyll fluorescence and flow cytometric analysis. *Ecol Indic* 78:131–141. https://doi.org/10.1016/j.ecolind.2017.03.008
14. Kana TM, Geider RJ, Critchley C (1997) Regulation of photosynthetic pigments in micro-algae by multiple environmental factors: a dynamic balance hypothesis. *New Phytol* 137:629–638. https://doi.org/10.1046/j.1469-8137.1997.00857.x
15. Li M, Shi X, Guo C, Lin S (2016) Phosphorus deficiency inhibits cell division but not growth in the dinoflagellate *Amphidinium carterae*. *Front Microbiol* 7:826.
16. Liu Y, Liu X, Nan F, Liu Q, Lv J, Feng J, Xie S (2024) Fe(III)-mediated changes in microalgae-associated bacterial communities and dissolved organic matter characteristics: A case study for *Chlorococcum* sp. GD. *Algal Res* 82:103637. https://doi.org/10.1016/j.algal.2024.103637
17. Malych R, Stopka P, Mach J, Kotabová E, Prášil O, Sutak R (2022) Flow cytometry-based study of model marine microalgal consortia revealed an ecological advantage of siderophore utilization by the dinoflagellate *Amphidinium carterae*. *Comput Struct Biotechnol J* 20:287–295. https://doi.org/10.1016/j.csbj.2021.12.020
18. Niedzwiedzki D, Jiang J, Lo C, Blankenship R (2013) Low-temperature spectroscopic properties of the Peridinin–chlorophyll a–protein (PCP) complex from the coral symbiotic dinoflagellate *Symbiodinium*. *J Phys Chem B* 117:11091–11099.
19. Novoveská L, Nielsen SL, Eroldoğan OT, Haznedaroglu BZ, Rinkevich B, Fazi S, Robbens J, Vasquez M, Einarsson H (2023) Overview and challenges of large-scale cultivation of photosynthetic microalgae and cyanobacteria. *Mar Drugs* 21:445. https://doi.org/10.3390/md21080445
20. Oh SJ, Kwon HK, Noh IH, Yang HS (2010) Dissolved organic phosphorus utilization and alkaline phosphatase activity of the dinoflagellate *Gymnodinium impudicum* isolated from the South Sea of Korea. *Ocean Sci J* 45:171–178.
21. Prézelin BB, Haxo FT (1976) Purification and characterization of Peridinin–chlorophyll a–proteins from the marine dinoflagellates *Glenodinium* sp. and *Gonyaulax polyedra*. *Planta* 128:133–141.
22. Qiu S, Yuan Y, Li X, Zhao C, He Y, Tang B, Wang W, Fan J (2023) Peridinin–chlorophyll a–protein complex industry from algae: a critical review of the current advancements, hurdles, and biotechnological potential. *Algal Res* 72:103118.
23. Salbitani G, Carfagna S (2021) Ammonium utilization in microalgae: a sustainable method for wastewater treatment. *Sustainability* 13:956.
24. Schoffman H, Lis H, Shaked Y, Keren N (2016) Iron-nutrient interactions within phytoplankton. *Front Plant Sci* 7:1223.
25. Schulte T, Magdaong NCM, Di Valentin M, Agostini A, Tait CE, Niedzwiedzki DM, Carbonera D, Hofmann E (2025) Structural and spectroscopic characterization of the Peridinin–chlorophyll a–

protein (PCP) complex from *Heterocapsa pygmaea* (HPPCP). *Biochim Biophys Acta Bioenerg* 1866:149510.

26. Shen A, Ma Z, Jiang K, Li D (2016) Effects of temperature on growth, photophysiology, Rubisco gene expression in *Prorocentrum donghaiense* and *Karenia mikimotoi*. *Ocean Sci J* 51:581–589.
27. Trigueros M, Ansotegui A, Orive E (2000) Remarks on morphology and ecology of recurrent dinoflagellate species in the estuary of Urdaibai (northern Spain). *Bot Mar* 43:93–103.
28. Trigueros M, Orive E (2001) Seasonal variations of diatoms and dinoflagellates in a shallow, temperate estuary, with emphasis on neritic assemblages. *Hydrobiologia* 444:119–133.
29. Wang Y, Coyne KJ (2024) Molecular insights into the synergistic effects of putrescine and ammonium on dinoflagellates. *Int J Mol Sci* 25:1306.
30. Yamashita K, Suzuki K, Tokunaga E (2026) Novel Insight into Pigment's Synthesis and Accumulation in Microalgae Under Environmental Stress. In: Pigments from Microalgae Handbook—Volume I: Biological Foundations, Environmental Influences and Analytical Methods. *Springer Nature* 1:185–212. https://doi.org/10.1007/978-3-031-93945-7_6
31. Zhang H, Gu B, Zhou Y, Ma X, Liu T, Xu H, Xie Z, Liu K, Wang D, Xia X (2022) Multi-omics profiling reveals resource allocation and acclimation strategies to temperature changes in a marine dinoflagellate. *Appl Environ Microbiol* 88:e0121322.
32. Černterová D, Galbraith DW (2021) Best practices in the flow cytometry of microalgae. *Cytometry A* 99:359–364.

Figures

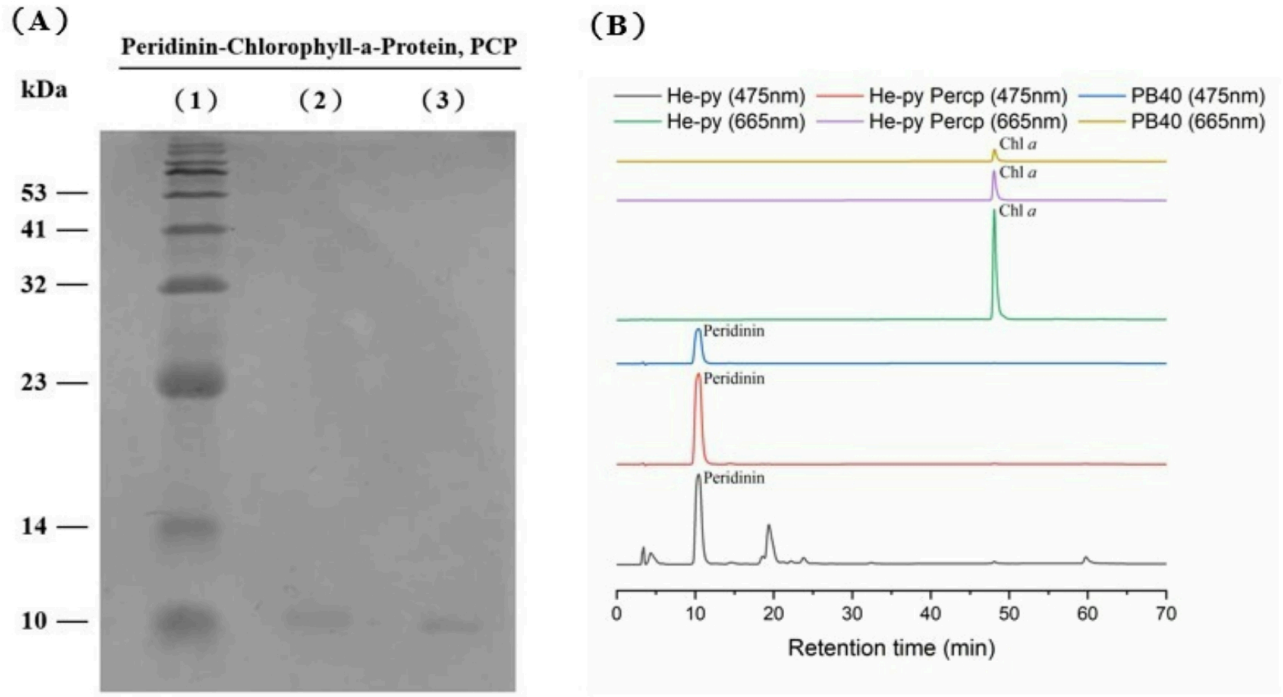


Figure 1

Characterization of peridinin–chlorophyll *a*–protein (PCP) in *Heterocapsa pygmaea*.

(A) SDS-PAGE profile showing a distinct protein band at approximately 10–15 kDa, corresponding to PCP.

(B) RP-HPLC chromatograms detected at 475 nm and 665 nm confirmed the characteristic pigment composition of PCP, including peridinin and chlorophyll *a*.

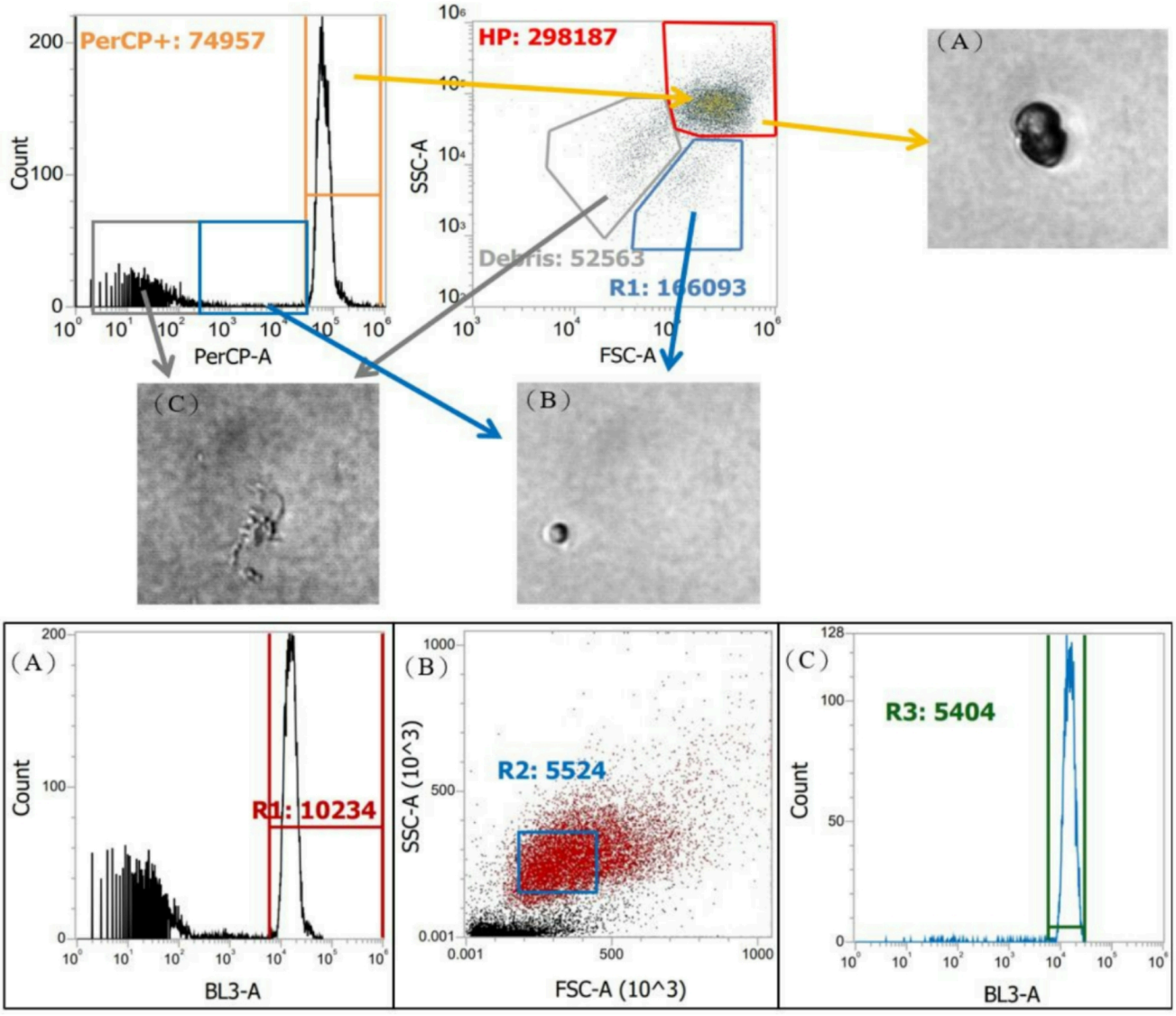


Figure 2

Flow cytometry-based analytical framework for assessing biomass and PCP-associated fluorescence in *Heterocapsa pygmaea*. The upper panels illustrate the sequential identification of *H. pygmaea* cells using PerCP-associated fluorescence, FSC–SSC discrimination, and microscopic validation of gated populations and excluded particles. The lower panels show the gating workflow used for downstream analysis, including (A) fluorescence gating in the BL3-A channel, (B) FSC–SSC discrimination of viable cells, and (C) final fluorescence gating of selected populations.

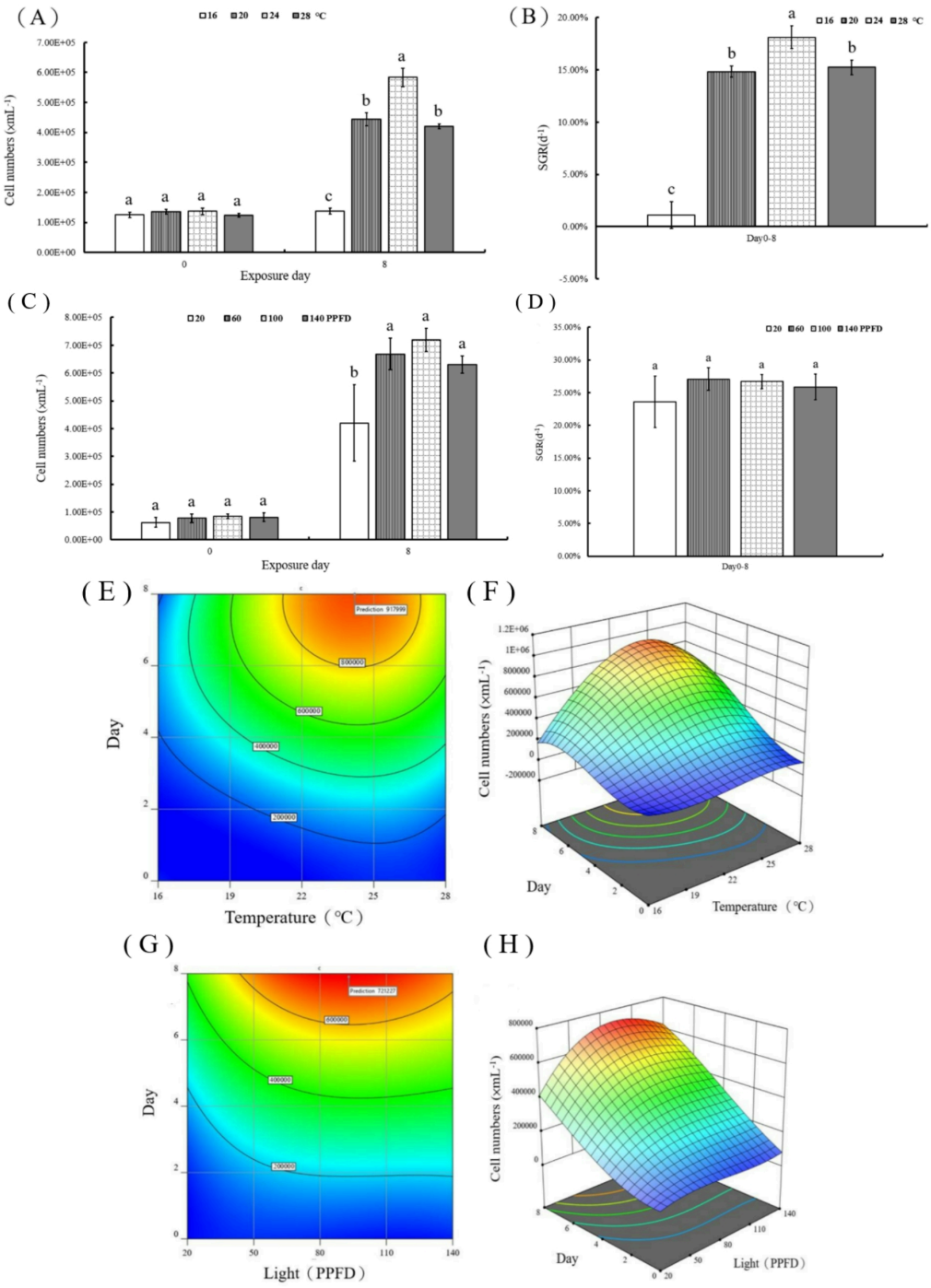


Figure 3

Effects of temperature and light intensity on the growth responses of *Heterocapsa pygmaea*.

(A–B) Cell density and specific growth rate (SGR) under different temperature conditions. (C–D) Cell density and SGR under varying light intensities. (E–F) Response surface contours and three-dimensional plots showing the effect of temperature on biomass production.

(G–H) Response surface contour and three-dimensional plots showing the effect of light intensity on biomass production.

Different letters indicate significant differences ($p < 0.05$).

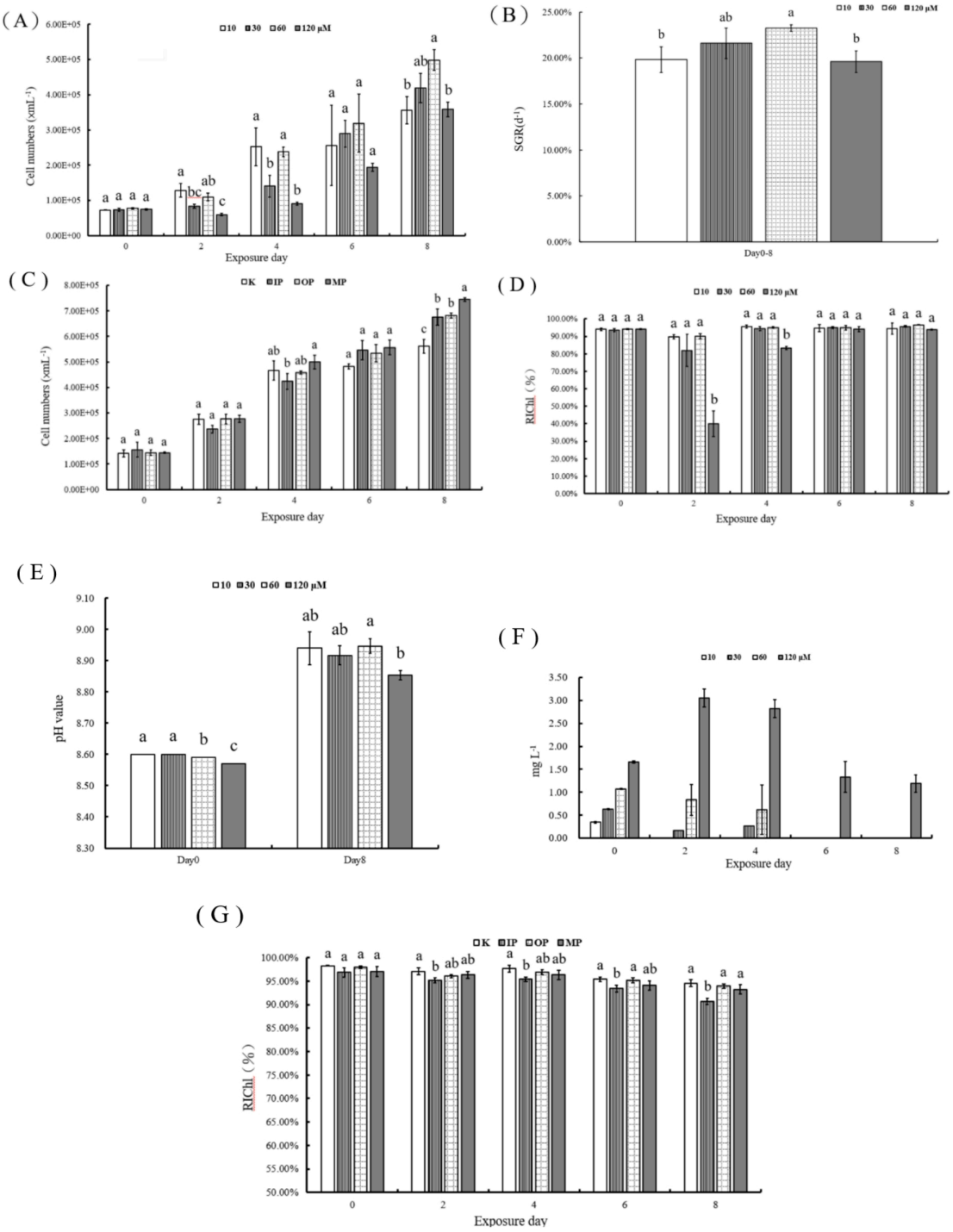


Figure 4

Effects of phosphorus concentration and source on growth, nutrient utilization, and relative fluorescence intensity in *Heterocapsa pygmaea*.

(A–B) Cell density and specific growth rate (SGR) under different phosphorus concentrations.

(C) Cell density responses to varying phosphorus concentrations throughout the cultivation period.

(D) Relative fluorescence intensity (a proxy for PCP-associated performance) under different phosphorus concentrations.

(E) pH variation during cultivation.

(F) Dynamics of total phosphorus depletion during cultivation.

(G) Relative fluorescence intensity under different phosphorus source treatments. Different letters indicate significant differences among treatments ($p < 0.05$).

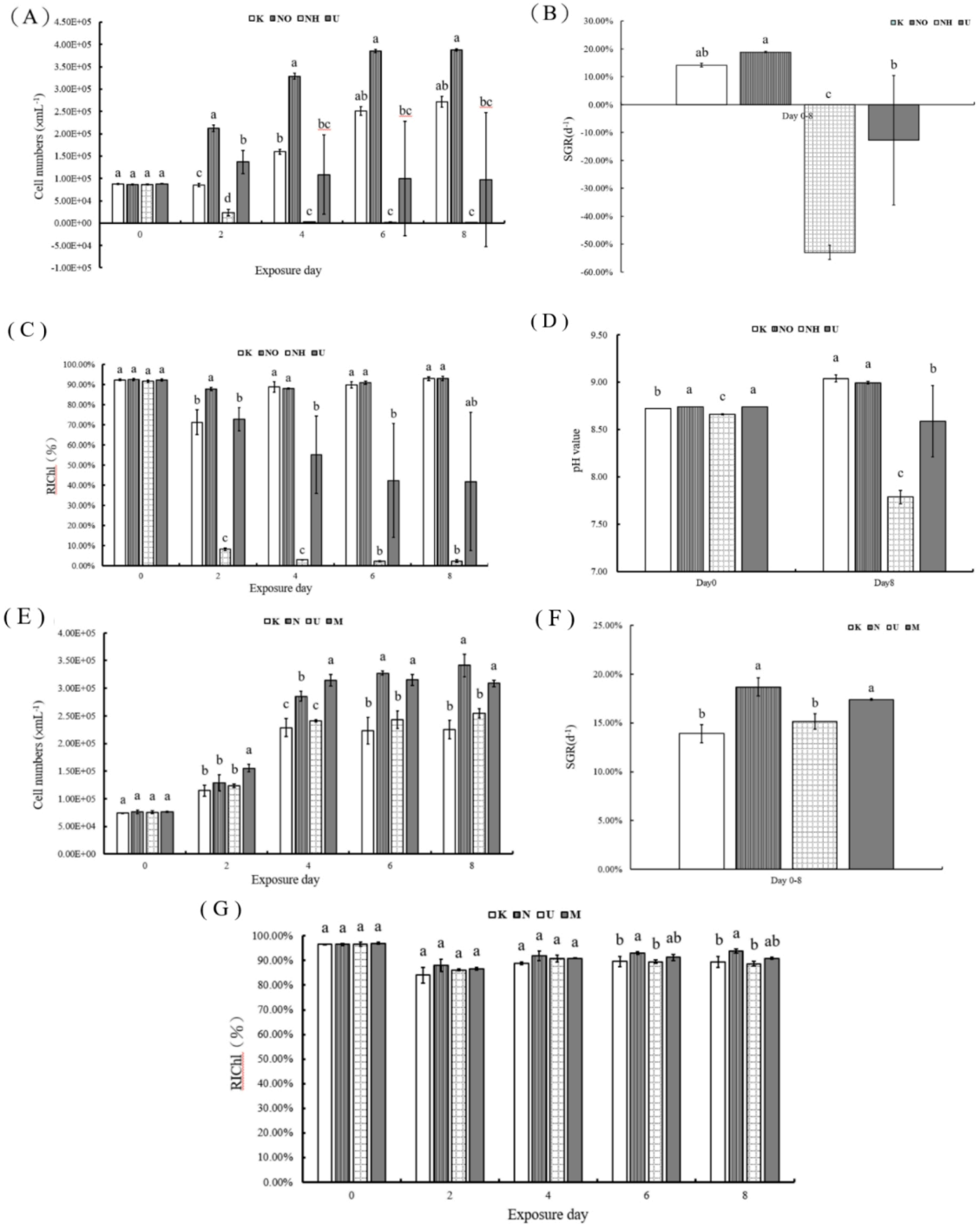


Figure 5

Effects of nitrogen source and nitrate–urea substitution strategy on growth and relative fluorescence intensity of *Heterocapsa pygmaea*.

(A–B) Cell density and specific growth rate (SGR) under different nitrogen source treatments. (C) Relative fluorescence intensity under different nitrogen source treatments. (D) pH variation during

cultivation. (E–F) Cell density and SGR under different nitrate–urea substitution treatments. (G)Relative fluorescence intensity under different nitrate–urea substitution treatments. Different letters indicate significant differences between treatments ($p < 0.05$).

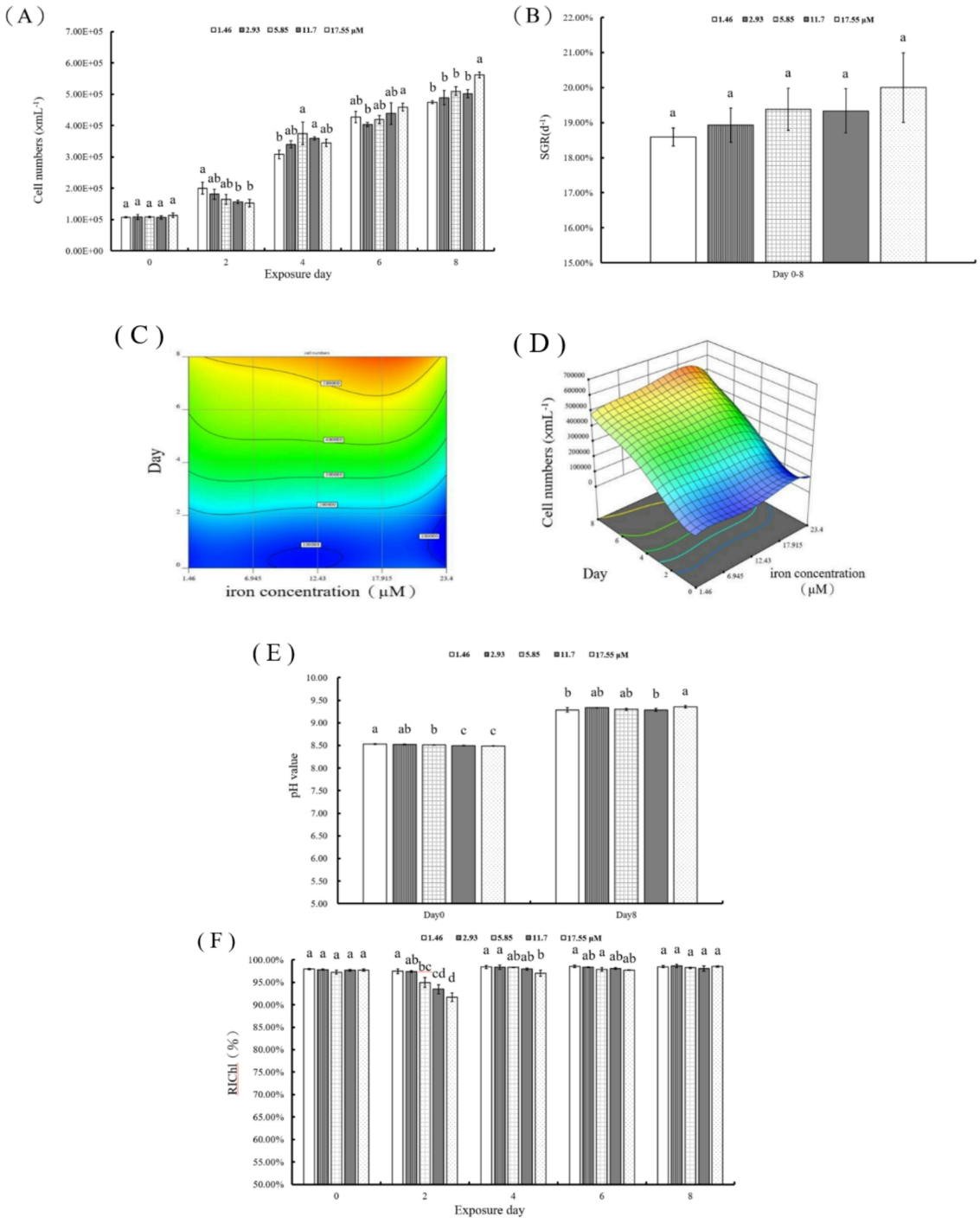


Figure 6

Effects of iron concentration on growth and PCP-associated performance in *Heterocapsa pygmaea*.

(A–B) Cell density and specific growth rate (SGR) under different iron concentrations. (C–D) Response surface contour and three-dimensional plots showing the effect of iron concentration on culture productivity. (E) pH variation during cultivation.

(F) Relative fluorescence intensity (a proxy for PCP-associated performance) under varying iron concentrations.

Different letters indicate significant differences between treatments ($p < 0.05$).

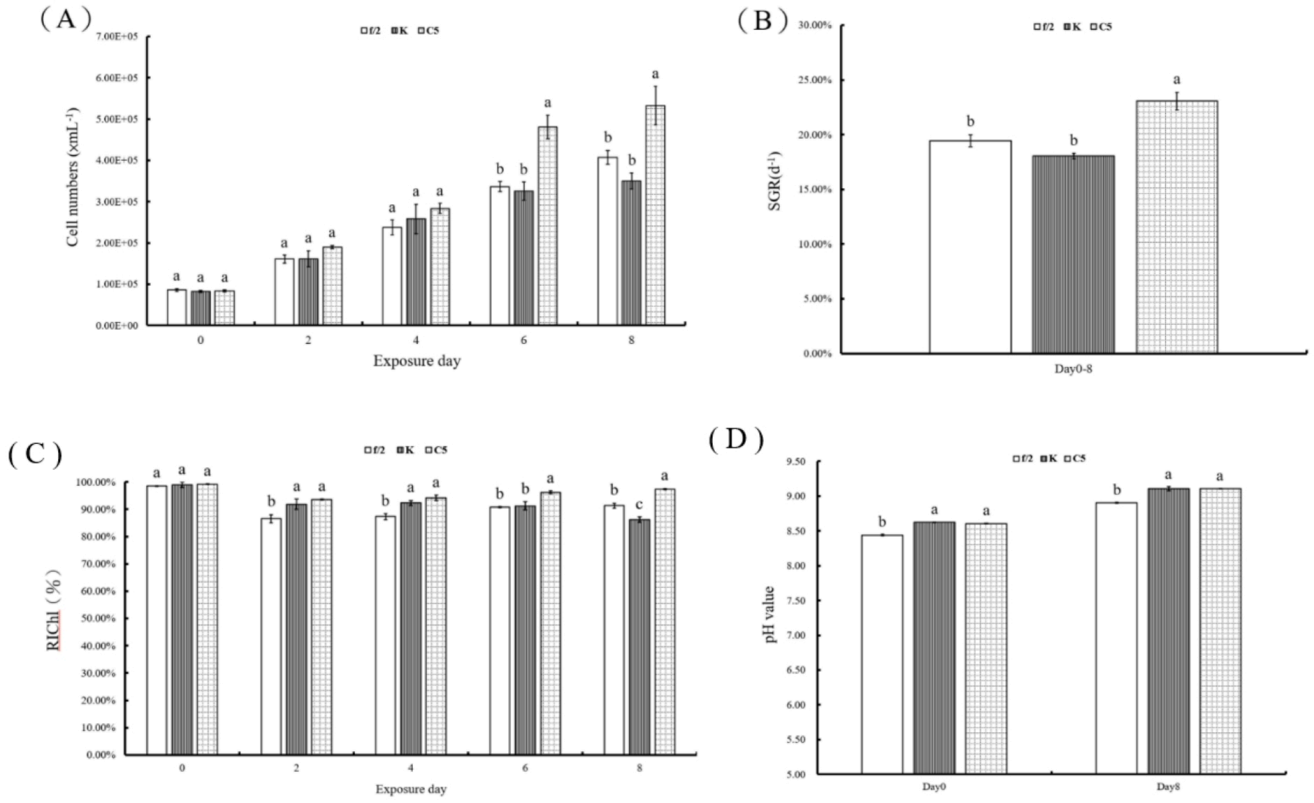


Figure 7

Validation of the optimized cultivation conditions using modified C5 medium.

(A–B) Comparison of cell density and specific growth rate (SGR) among C5, f/2, and K media. (C) Relative fluorescence intensity (a proxy for PCP-associated performance) under different culture media. (D) pH variation during cultivation.

Different letters indicate significant differences between treatments ($p < 0.05$).

Supplementary Files

This is a list of supplementary files associated with this preprint. Click to download.

- SUPPLEMENTARYMATERIALS.docx
- floatimage1.jpeg